Eur. Phys. J. B **31**, 69–74 (2003)
DOI: 10.1140/epjb/e2003-00010-2

THE EUROPEAN PHYSICAL JOURNAL B

Exchange coupling in ultrathin epitaxial yttrium iron garnet films

E. Popova[1,2,a], N. Keller[1], F. Jomard[3], L. Thomas[1], M.-C. Brianso[4], F. Gendron[5], M. Guyot[1], and M. Tessier[1]

[1] LMOV, UVSQ-CNRS, bâtiment Fermat, 45 avenue des États-Unis, 78035 Versailles Cedex, France
[2] Institute of Magnetism NASU, 36[b] Vernadsky Blvd., Kyiv, 03142, Ukraine
[3] LPSC, CNRS, 1 place Aristide Briand, 92195 Meudon Cedex, France
[4] Département de Physique, UVSQ, bâtiment E, 45 avenue des États-Unis, 78035 Versailles Cedex, France
[5] LMDH, Université Pierre et Marie Curie, Boite 86, 4, place Jussieu, 75252 Paris Cedex 05, France

Received 3 June 2002 / Received in final form 7 October 2002
Published online 27 January 2003 –

Abstract. Magnetic exchange coupling has been observed for ultrathin films of yttrium iron garnet ($Y_3Fe_5O_{12}$ or YIG). Single-crystalline YIG films were prepared on yttrium aluminium garnet ($Y_3Al_5O_{12}$ or YAG) substrates by pulsed laser deposition. (111) and (110) oriented substrates were used. Film thicknesses were varied from 180 Å to 4600 Å. Epitaxial growth of YIG on YAG was obtained in spite of the lattice mismatch of 3%. Magnetic hysteresis loops recorded for ultrathin YIG films have a "bee-waist" shape and show a coupling between two different magnetic phases. The first phase is magnetically soft YIG. A composition study by secondary ion mass spectroscopy shows the second phase to be $Y_3Fe_{5-x}Al_xO_{12}$ due to the interdiffusion of Fe and Al at the film/substrate interface. This compound is known to be magnetically harder and to have weaker magnetization than YIG. The coupling of the two phases leads to a hysteresis loop displacement at low temperatures. This displacement varies differently with film thickness for two substrate orientations. Assuming an interfacial coupling, the maximal interaction energy is estimated to be about 0.17 erg/cm^2 at 5 K for (111) oriented sample.

PACS. 75.60.Ej Magnetization curves, hysteresis, Barkhausen and related effects – 75.60.Jk Magnetization reversal mechanisms – 75.70.Ak Magnetic properties of monolayers and thin films

1 Introduction

Low dimensionality effects in thin films are of great interest for fundamental science and applications. Recently much attention has been paid to ultrathin metallic magnetic films, whose magnetic properties exhibit numerous changes compared to bulk magnetic properties [1]. Thin magnetic oxides, and in particular ferrite films, are also of increasing interest due to their various technical applications (see for example Ref. [2,3]).

Yttrium iron garnet ($Y_3Fe_5O_{12}$ or YIG) has been extensively studied in bulk and thick film (thickness $t > 1$ μm) samples (Ref. [4] and references therein). We choose YIG as a model material to investigate the changes of a magnetic oxide properties as a consequence of reduced thickness.

The "classical" substrate for the deposition of single crystalline YIG films is gadolinium gallium garnet ($Gd_3Ga_5O_{12}$ or GGG) [4]. The lattice mismatch between GGG and YIG is about 0.1%. This allows the growth of single-crystalline epitaxial films of good quality. Unfortunately, GGG is a strong paramagnet, and is therefore not suitable for the detection of the weak magnetic signal arising from ultrathin YIG films. An alternative could be a diamagnetic garnet substrate such as yttrium aluminium garnet ($Y_3Al_5O_{12}$ or YAG). However, epitaxial growth is expected to be difficult due to a significant lattice mismatch for this material. The YAG lattice parameter is 12.005 Å, which is 3% smaller than the size of the YIG unit cell (12.376 Å).

2 Film preparation

Thin and ultrathin YIG films were prepared by pulsed laser deposition on single crystalline yttrium aluminium garnet substrates of (111) and (110) orientation. Film thicknesses were varied between 180 Å and 4600 Å.

A polycrystalline YIG target was ablated by the third harmonic (355 nm) of a Nd:YAG laser. The laser beam was displaced on the target surface by means of the computer-controlled XY-scanner. The pulse length of the laser was 6 ns at a repetition rate of 10 Hz and maximum energy 180 mJ/pulse. The laser fluency was

[a] Presently at LPM, Université H. Poincaré, BP 239, 54506 Vandœuvre-lès-Nancy
e-mail: popova@lpm.u-nancy.fr

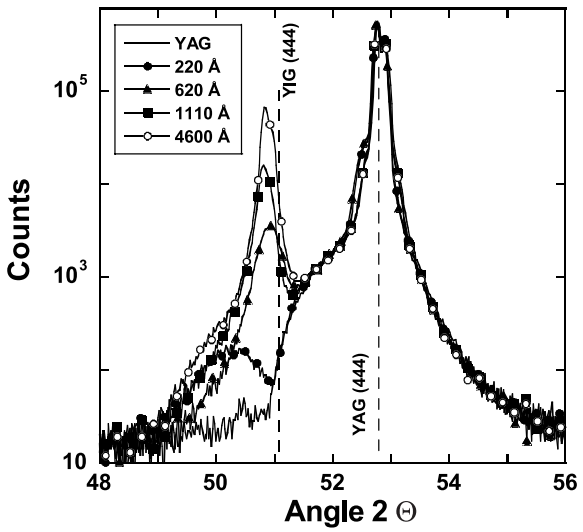

Fig. 1. X-ray diffraction diagrams of YIG thin and ultrathin films deposited on (111) YAG substrates. Dotted lines show the positions of the (444) diffraction peaks of the YAG substrate and the YIG target.

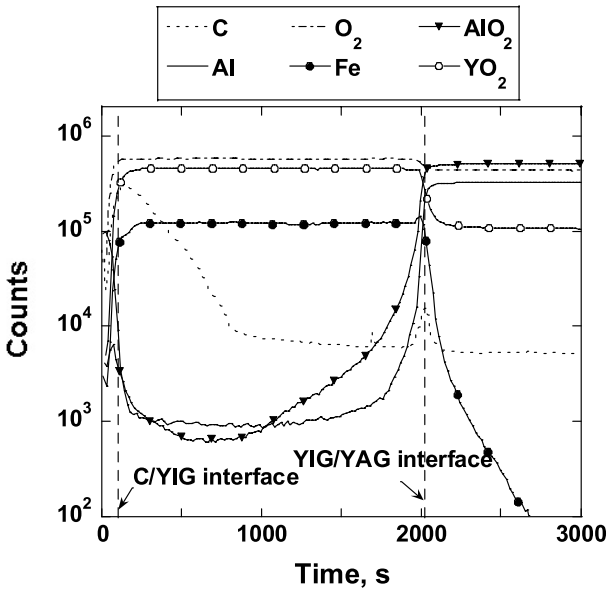

Fig. 2. Concentration profiles of ions and aggregates throughout the entire film and a part of the substrate. Dotted lines show the position of the interfaces carbon/YIG and YIG/substrate in a YIG film of thickness of 4600 Å. SIMS analysis was performed with a Cs – ion source.

around 8 J/cm^2 and the substrate temperature T_S was kept close to 660 °C. The deposition was carried on in a partial oxygen pressure P_{O_2} of 30 mTorr. The films were not annealed after the deposition. The target to substrate distance was 50 mm.

In spite of the significant lattice mismatch between YIG and YAG, all films were single-crystalline and epitaxial as proved by cross-section transmission electron microscopy [5]. Figure 1 shows the evolution of the (444) diffraction peak as a function of film thickness. The perpendicular lattice spacing of the first ten YIG monolayers (120 Å) is close to that of YAG. This can be deduced from the slight shift of the diffraction peak corresponding to the (111) orientation of YAG to the smaller angles, *i.e.* to the bigger lattice parameters. The perpendicular lattice parameter of these first YIG layers is about 12.011 Å. The relative lattice match of this layer to YAG is due to diffusion of Al from the substrate into the film as will be shown in Section 3. The partial substitution of Fe by smaller Al atoms is more important near the film/substrate interface, and, consequently, the lattice spacing of first ten substituted YIG layers is closer to that of YAG substrate.

The concentration of aluminium in YIG film decreases gradually with increasing film thickness. Finally, for films exceeding a thickness of typically 120 Å to 150 Å, a pure YIG is formed on top of the substituted $Y_3Fe_{5-x}Al_xO_{12}$ layer. Because of the lattice mismatch, the YIG film is compressed in-plane, and a Poisson expansion in the out-of-plane direction is observed (see the curve for 220 Å-thick sample on Figure 1, where the lattice parameter is about 1.4% larger than bulk lattice spacing). Then the film starts to relax towards the bulk lattice parameter. However, a slight out-of-plane expansion of about 0.4% remains even at 4600 Å because of the residual stresses.

3 Film structure

As the films are deposited at an elevated temperature, an interdiffusion between Fe and Al at the film/substrate interface becomes possible. Consequently, a layer of $Y_3Fe_{5-x}Al_xO_{12}$ can be formed, with x changing gradually from 5 to 0 within the film. The counts of the secondary ions emitted from the sample after its bombardment by Cs^+ ions are presented in Figure 2. Different elements (C, Al, Fe) and aggregates (O_2, AlO_2, YO_2) were traced in order to ensure a precise profiling of the film composition. The abrasion was performed throughout the entire thickness of the film and through a part of the substrate. The significant quantity of carbon ions on the surface of the sample is due to the presence of a conducting carbon coating. This layer was deposited on the surface of YIG to evacuate the charges induced by the beam of primary ions. The dashed line marks the position of the interface between the film and the substrate. The interface was reached when the intensity of the signals resulting from iron (aluminium) decreased (increased) to 50% of its maximum value. Besides, a significant increase of the quantity of carbon ions was detected; this corresponds to a slight pollution of the substrate surface before the deposition.

From Figure 2 it is clear that the cation ratio Y / Fe is constant through all the film, which confirms the good film quality. The quantity of iron ions decreases when the primary ions penetrate into the substrate, and on the contrary, the quantity of aluminium increases.

To clarify the problem of the interdiffusion, the depth of the crater created by the bombardment of the sample was measured. This allows to calculate the abrasion

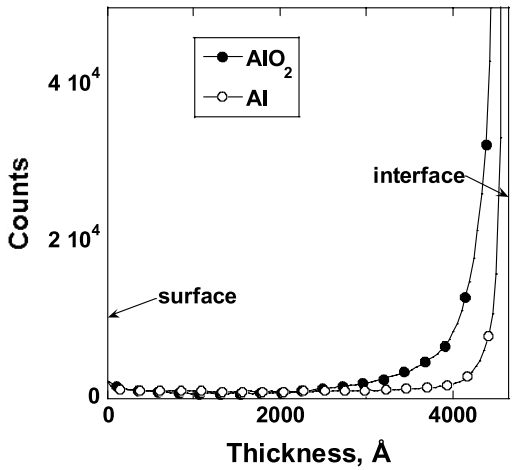

Fig. 3. Aluminium ion and aluminium oxide concentration as a function of a film thickness. The measurements are performed from the film surface (0 Å) to its interface with a substrate (4600 Å). The film was deposited at 650 °C during 12 hours.

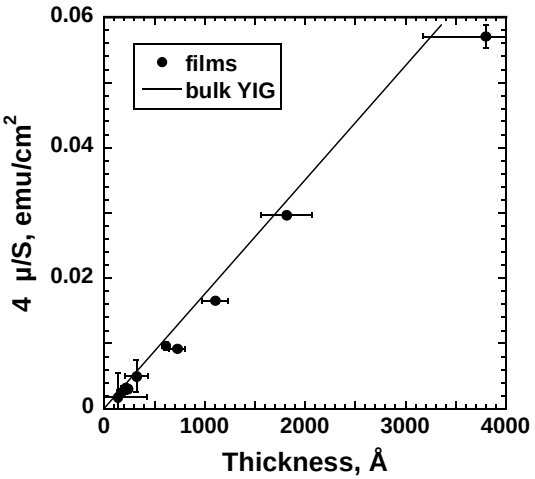

Fig. 4. Magnetic moment per unit surface area for films of different thickness measured by SQUID at 300 K. The solid line represents the expected variation for $4\pi M_S = 1780$ G.

rates of YIG and YAG, which are indeed different, and the relative thickness of the aluminium diffusion into a film. Figure 3 represents the counts of detected Al ions and AlO_2 aggregates throughout the thickness of a film, from the surface (0 Å) to the interface with YAG (4600 Å). It would appear that aluminium penetrates into the YIG film on a thickness of about 600 Å for a film deposited at 650 °C over a 12 hours period. As the depth of the diffusion at a given temperature is proportional to the square root of the time of deposition [6], one can calculate the thickness of $Y_3Fe_{5-x}Al_xO_{12}$ layer to be 100 Å in a ultrathin film of 200 Å.

YIG substituted by Al has been extensively studied in the past [7–11], and is known to have a weak magnetization and high coercivity compared to bulk YIG. In pure $Y_3Fe_5O_{12}$ crystal there are tree tetrahedral and two octahedral positions per formula unit occupied by iron ions, forming two antiparallel magnetic sublattices [8]. The magnetic moments of two Fe^{3+} on octahedral positions are compensated by moments of two Fe^{3+} onto tetrahedral positions, leaving one uncompensated iron moment on a tetrahedral site. The substitution of Fe^{3+} by diamagnetic Al^{3+} ions is possible in the full range of concentrations in $Y_3Fe_{5-x}Al_xO_{12}$ [10]. Al^{3+} ions can replace Fe^{3+} ions on octahedral and tetrahedral sites. However, for most of the composition range x these Al^{3+} ions have a preference for the tetrahedral sites [8–11]. This can be explained qualitatively by the fact that the octahedral positions provide a larger volume than the tetrahedral sites. Therefore, the smaller aluminium ions preferentially occupy the smaller tetrahedral positions. As the resulting magnetic moment of YIG comes from uncompensated moment of iron ion in tetrahedral position, the substitution of Fe^{3+} by Al^{3+} leads to the formation of a ferrimagnetic layer with reduced magnetization or of a compensated antiferromagnetic layer depending on the concentration x of aluminium ions. In the particular case of formation of substituted YIG by diffusion, x changes gradually from 5 to 0 starting from the substrate. Consequently, the resulting magnetization of $Y_3Fe_{5-x}Al_xO_{12}$ is smaller than pure YIG magnetization. As a result, the magnetization per unit volume of a whole film should be lower than the magnetization of a pure YIG film.

The magnetic moment per unit surface area $4\pi\mu/S$ is presented in Figure 4 as a function of the film thickness t. The solid line represents the variation of the magnetic moment expected for YIG with $4\pi M_S = 1780$ G. Indeed, the magnetization of the films is lower than the value expected for "ideal" bulk-like YIG films. Note that this reduced magnetization can not be caused by the presence of a "dead layer", since its contribution would be more significant in the ultrathin films than in thicker films, which is not observed in the experiments.

4 Exchange coupling

Apart from the reduced saturation magnetization, we observe another interesting magnetic effect in the YIG / YAG films. This relates to the particular shape of the hysteresis loop in ultrathin film called "bee-waist" which exhibits almost zero coercive field (Fig. 5a). The appearance of such a kind of hysteresis loop suggests the coupling of two magnetic phases, one hard and another soft. They could be either exchange coupled at the interface [12], or the magnetically soft material may be affected by the demagnetizing field of the hard material [13,14].

4.1 Room temperature

The hysteresis loops at room temperature for two films with different thickness are presented in Figure 5. The field applied during the measurement is oriented parallel to the plane of a film. The "bee-waist" shaped hysteresis loop is observed for the ultrathin films only (Fig. 5a).

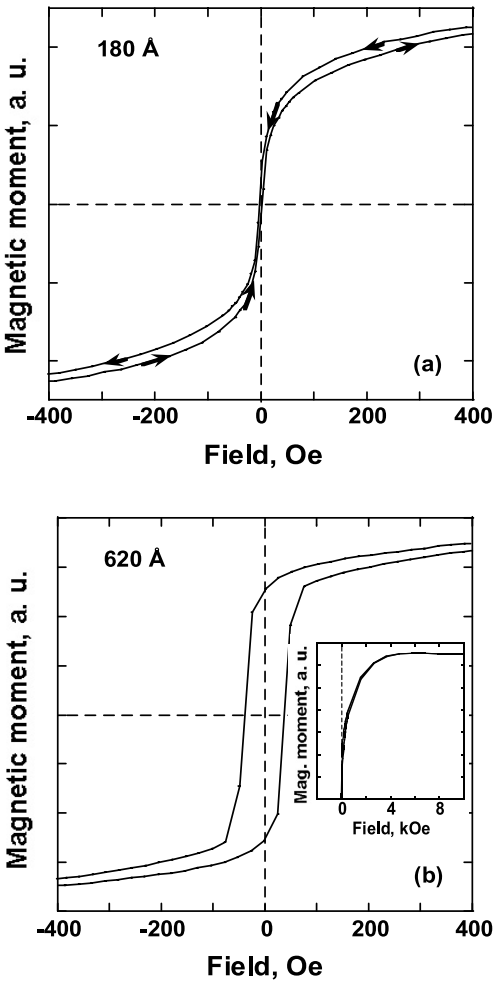

Fig. 5. Hysteresis loops recorded at 300 K for films of thickness: (a) 180 Å, (b) 620 Å. The magnetization was saturated with an in-plane applied field of 10 000 Oe. Inset to Figure 5b shows the saturation of the sample in positive field.

When the film thickness is increased, the hysteresis loop exhibits the usual shape (Fig. 5b). However, as shown on inset to Figure 5b, the saturation of the sample takes place in high fields (∼4000 Oe), even though the coercivity is quite low (25 Oe, Fig. 5b). This can be described with the presence of two magnetic phases: a magnetically soft phase ($Y_3Fe_5O_{12}$) and the other one magnetically hard ($Y_3Fe_{5-x}Al_xO_{12}$), as is pointed out previously. The soft magnetic phase has a saturation magnetization close to that of the YIG and a weak coercivity of a dozen Oersted. This magnetic phase dominates in rather thick films ($t > 1000$ Å). The second phase has a weaker magnetization and a stronger coercivity, about a few times larger than soft phase.

The presence of two coupled magnetic phases is confirmed by ferromagnetic resonance (FMR) measurements of ultrathin films. Figure 6 shows the FMR spectrum recorded in applied field parallel to the film plane. Two resonance peaks close to each other are observed. They

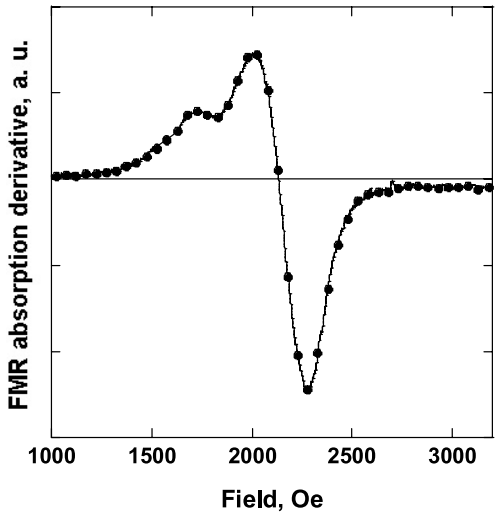

Fig. 6. FMR absorption spectrum for the ultrathin film (220 Å) at 300 K. The applied static magnetic field is oriented in the plane of a film.

shift coherently with the change of the angle between the applied dc magnetic field and the film plane. This behaviour is most often attributed to the presence of two coupled magnetic phases with different magnetization and/or anisotropy (see Ref. [15] and references therein). The two peak intensities for an ultrathin film are comparable, *i.e.* the quantity of two magnetic phases in this film are almost identical. That is consistent with Al diffusion lengths estimation from SIMS measurements indicating for this sample of 220 Å the thickness of the hard phase to be about 120 Å.

4.2 Low temperature

The "bee-waist" shaped hysteresis is observed in the measurement range between 300 K to 240 K. When the temperature is decreased, the coercive field of the soft and hard layers increase, as the anisotropy constants increase. At a certain temperature which depends on the thickness of the YIG film, the coercivity of the soft layer increases above a critical value and the hysteresis loop exhibits the usual shape. The hysteresis curves are symmetric with respect to zero field for the temperatures between 300 K and 75 K.

The magnetic exchange coupling is observed at lower temperature by the hysteresis loop displacement (see the inset to Fig. 7). When the sample is first saturated in a positive magnetic field, the hysteresis loop is shifted towards negative fields. This is a "standard" exchange bias behaviour of a two-layer antiferromagnetic-ferro(ferri)magnetic system [12]. As the resulting magnetic moment of YIG originates from the non-compensated iron moments in the tetrahedral sites, and since the non-magnetic Al ions occupy preferentially the tetrahedral positions, it is possible to obtain a compensated antiferromagnetic layer at a certain aluminium concentration in a

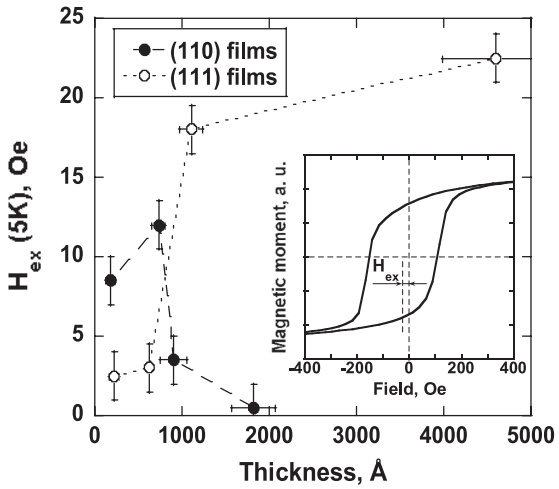

Fig. 7. Exchange field H_{ex} at 5 K as a function of the film thickness for two substrate orientations (110) and (111). Dotted lines are guides to the eye. The inset shows the hysteresis loop displacement at 5 K for a (111)-oriented sample with a thickness of 4600 Å.

YIG film [9]. This layer can serve as a pinning film for the pure YIG.

The measurements of the loop displacement, that we shall call the exchange field H_{ex} as in the classical case of exchange bias, were carried out in a SQUID magnetometer after a field cool procedure. We should stress that there was no difference neither in the loop shape, nor in its position between zero field cool and field cool procedure.

The exchange field depends on the film thickness. As shown in Figure 7, the exchange field exhibits considerably different thickness variations for two substrate orientations (111) and (110). While the exchange field decreases with increasing film thickness for (110) oriented films as predicted by the existing models [12], it seems to increase for (111) oriented samples. One of the reasons for this atypical behaviour could be related to the film growth mode and the resulting interfacial roughness. Indeed, the growth mode is different for two substrate orientations due to the lattice strains. It has been observed [5] that YIG exhibits columnar growth on both types of YAG substrates. In the vicinity of the film/substrate interface the columns are separated by small fractions of poorly crystallised zones for the (111) oriented films. The (110) samples are much better crystallised than those prepared on (111) substrates. This structural arrangement certainly modifies the coupling strength of (111) samples in comparison to (110) ones. For the ultrathin films the decrease of H_{ex} is accompanied by a significant increase of the film coercivity. This is most probably related to the presence of the imperfections in the hard layer as described in reference [16].

The thermal variation of H_{ex} gives a significant indication concerning the type of coupling present in this two-layer system. The two possibilities discussed earlier are either a dipolar coupling or a pure exchange coupling. In the case of a dipolar coupling, the strength of the coupling should be roughly proportional to the product of the saturation magnetizations of the two magnetic sublayers, YIG and $Y_3Fe_{5-x}Al_xO_{12}$. Moreover, the thermal variation of dipolar coupling should be essentially related to the thermal variation of the saturation magnetization, which is $\delta M_S/M_S(300\ \mathrm{K}) \sim 38\%$ for YIG in the 5 K to 300 K temperature range. However, the bias field decreases strongly upon increasing the temperature, and vanishes above 75 K. This disparity between $M_S(T)$ and $H_{ex}(T)$ is an indication that H_{ex} does not originate from dipolar coupling, but from an exchange interaction.

Assuming exchange coupled layers with a flat interface, the coupling energy [12] can be roughly estimated as $E_{ex} \sim H_{ex}M_S t \approx 0.17\ \mathrm{erg/cm^2}$ at 5 K for the sample of (111) orientation showing the highest value of H_{ex}. This value is comparable to E_{ex} obtained for antiferroferrimagnetic $NiO/NiFe_2O_4$ system [17]. For the (110) oriented films the maximal coupling energy is about 20 times lower in the thickness range from 180 to 1820 Å.

A "bee-waist" hysteresis loop and the loop displacement were not observed when the applied field was perpendicular to the surface of the film. This result is predictable as the easy magnetization axis of both layers is "in-plane". It is also worth noticing that, contrary to the case of ultrathin polycrystalline YIG films [15], the spontaneous magnetization always remains "in-plane" regardless of the temperature.

5 Conclusions

Single-crystalline epitaxial YIG films were grown on yttrium aluminium garnet substrates by pulsed laser deposition. A "bee-waist" shape of the hysteresis loop was observed for ultrathin YIG / YAG films at room temperature. This effect can be explained by a magnetic exchange coupling between two magnetic phases, an interfacial hard phase and a soft phase. The soft phase is pure YIG. The hard phase, $Y_3Fe_{5-x}Al_xO_{12}$, with low magnetization is formed as a consequence of a slight interdiffusion of Fe and Al at the film/substrate interface. The overall film magnetization is therefore reduced in comparison to that of "bulk" YIG of similar thickness. The shape of the hysteresis loops depend on film thickness and temperature.

At low temperature a hysteresis loop shift is observed. The value of the displacement field depends on the film thickness, and varies differently for two sample orientations (110) and (111). One of the reasons of such a behaviour can be the difference in the growth modes and crystallisation of these two types of films. From the experimental data we estimate the maximal interface exchange energy for (111) oriented samples in the thickness range from 220 to 4600 Å to be around $0.17\ \mathrm{erg/cm^2}$ at 5 K.

The thermal variation of the saturation magnetization compared to the observed variation of H_{ex} demonstrates that the coupling is not due to the demagnetizing fields.

No reorientation of the magnetization perpendicularly to the film surface is observed between 5 K to 300 K, contrary to the case of polycrystalline YIG films [15].

References

1. B. Heinrich, J.F. Cochran, Adv. Phys. **42**, 523 (1993)
2. J.D. Adam, S.V. Krishnaswamy, S.H. Talisa, K.C. Yoo, J. Magn. Magn. Mater. **83**, 419 (1990)
3. F.J. Rachford, M. Levy, R.M. Osgood Jr., A. Kumar, H. Bakhru, J. Appl. Phys. **85**, 5217 (1999)
4. Landolt-Börnstein, *Numerical data and functional relationships in science and technology*, Vol. 12, *Magnetic and other properties of oxides and related compounds: garnets and perovskites*, edited by K.-H. Hellwege (Springer-Verlag Berlin, 1978), 500 pp.
5. E. Popova, N. Keller, B. Mercey (to be published)
6. W. Lojkowski, H.-J. Fecht, Progr. Mater. Science **45**, 339 (2000)
7. B.E. Rubinshtein, Bull. Acad. Sci. URSS, Phys. Ser. (English Transl.) **35**, 1006 (1971)
8. M.A. Gilleo, S. Geller, Phys. Rev. B **110**, 73 (1958)
9. P. Fischer, W. Hälg, P. Roggwiller, E.R. Czerlinsky, Solid State Comm. **16**, 987 (1975)
10. D. Rodic, M. Mitric, R. Tellgren, H. Rundlof, J. Magn. Magn. Mater. **232**, 1 (2001)
11. P. Görnert, C.G. d'Ambly, Phys. Stat. Sol. (a) **29**, 95 (1975)
12. J. Nogués, I.K. Schuller, J. Magn. Magn. Mater. **192**, 203 (1999)
13. A. Aharoni, J. Appl. Phys. **76**, 6977 (1994)
14. Patent *Magnetic Memory Array with Magnetic Tunnel Junction Memory Cells Having Flux-Closed Free Layers*, S.S. Parkin, L. Thomas, issued as patent number 6166948 by US Patent and Trademark Office, December 26, 2000
15. E. Popova, N. Keller, F. Gendron, M. Guyot, M.-C. Brianso, Y. Dumond, M. Tessier, J. Appl. Phys. **90**, 1422 (2001)
16. J.-V. Kim, R.L. Stamps, Appl. Phys. Lett. **79**, 2785 (2001)
17. B. Negulescu, L. Thomas, Y. Dumont, M. Tessier, N. Keller, M. Guyot, J. Magn. Magn. Mater. **242-245**, 529 (2002)